SCIENTIFIC REPORTS

OPEN

SUBJECT AREAS:
TWO-DIMENSIONAL MATERIALS
MATERIALS CHEMISTRY

Received
1 October 2014

Accepted
31 December 2014

Published
27 January 2015

Correspondence and requests for materials should be addressed to B.C. (bjcho@kims.re.kr); M.G.H. (mghahm@kims.re.kr) or D.-H.K. (dhkim2@kims.re.kr)

* These authors contributed equally to this work.

Charge-transfer-based Gas Sensing Using Atomic-layer MoS_2

Byungjin Cho[1]*, Myung Gwan Hahm[1]*, Minseok Choi[2], Jongwon Yoon[3], Ah Ra Kim[1], Young-Joo Lee[1], Sung-Gyu Park[1], Jung-Dae Kwon[1], Chang Su Kim[1], Myungkwan Song[1], Yongsoo Jeong[4], Kee-Seok Nam[1], Sangchul Lee[5], Tae Jin Yoo[3], Chang Goo Kang[6], Byoung Hun Lee[3], Heung Cho Ko[3], Pulickel M. Ajayan[7] & Dong-Ho Kim[1]

[1]Advanced Functional Thin Films Department, Surface Technology Division, Korea Institute of Materials Science (KIMS), 797 Changwondaero, Sungsan-Gu, Changwon, Gyeongnam 642-831, Republic of Korea, [2]Advanced Characterization and Analysis Group, Korea Institute of Materials Science (KIMS), 797 Changwondaero, Sungsan-Gu, Changwon, Gyeongnam 642-831, Republic of Korea, [3]School of Materials Science and Engineering, Gwangju Institute of Science and Technology (GIST), 261 Cheomdan-gwagiro, Buk-Gu, Gwangju 500-712, Republic of Korea, [4]Electrochemistry Department, Korea Institute of Materials Science (KIMS), 797 Changwondaero, Sungsan-Gu, Changwon, Gyeongnam 642-831, Republic of Korea, [5]Department of Chemical Engineering and Materials Science, Stevens Institute of Technology, Hoboken, New Jersey 07030, United States, [6]Cambridge Graphene Center, University of Cambridge, 9 JJ Thomson Avenue, Cambridge, United Kingdom, [7]Department of Materials Science and NanoEngineering, Rice University, 6100 Main Street, Houston, Texas 77005, USA.

Two-dimensional (2D) molybdenum disulphide (MoS_2) atomic layers have a strong potential to be used as 2D electronic sensor components. However, intrinsic synthesis challenges have made this task difficult. In addition, the detection mechanisms for gas molecules are not fully understood. Here, we report a high-performance gas sensor constructed using atomic-layered MoS_2 synthesised by chemical vapour deposition (CVD). A highly sensitive and selective gas sensor based on the CVD-synthesised MoS_2 was developed. *In situ* photoluminescence characterisation revealed the charge transfer mechanism between the gas molecules and MoS_2, which was validated by theoretical calculations. First-principles density functional theory calculations indicated that NO_2 and NH_3 molecules have negative adsorption energies (i.e., the adsorption processes are exothermic). Thus, NO_2 and NH_3 molecules are likely to adsorb onto the surface of the MoS_2. The *in situ* PL characterisation of the changes in the peaks corresponding to charged trions and neutral excitons via gas adsorption processes was used to elucidate the mechanisms of charge transfer between the MoS_2 and the gas molecules.

Over the past few decades, metal oxide semiconductors have been applied as conventional chemical sensing materials because of their high sensitivity and relatively low cost[1–3]. However, they still have some critical drawbacks. First, metal oxide semiconductors exhibit poor sensitivity and selectivity at room temperature. This obstacle has led to the development of alternative materials such as carbon nanotubes[4], graphene[5], and transition metal dichalcogenides (TMDs)[6–11]. Recently, 2D TMDs have attracted much attention for use in next-generation nanoelectronic devices[12–14], with a single-layer MoS_2 transistor having been reported to exhibit outstanding performance[15]. The intrinsic merits of TMDs, including their high surface-to-volume ratio and semiconducting properties, have accelerated the development of a diverse range of applications of these materials as chemical sensors. A recent flurry of research involving MoS_2-based gas detection has mitigated the wide chasm between metal oxide materials and alternatives[6–11]. However, the fundamental mechanism of chemical sensing using MoS_2 remains unclear, limiting its practical applications. Here, we demonstrate highly sensitive and selective gas detection of NO_2 and NH_3 using uniform wafer-scale MoS_2 nanofilms synthesised by thermal chemical vapour deposition (CVD). We elucidate the charge transfer mechanism of MoS_2 gas adsorption using *in situ* photoluminescence (PL) and computational calculations involving first-principles density functional theory. The peak intensities from the positively charged trions (A^+) and neutral excitons (A^0) in the PL spectrum show trade-off phenomena by adsorption of each different gas molecule (NO_2 or NH_3) onto the MoS_2. The electron depletion of MoS_2 by NO_2 adsorption leads to an increase in the intensity of the A^+ peak and a suppression of the intensity of the A^0 peak, whereas electron accumulation by NH_3 adsorption suppresses the intensity of the A^+ peak and increases the intensity of the A^0 peak. These *in situ* PL characterisation results clarify the mechanisms of

charge transfer between the MoS_2 and the gas molecules. These findings will help to implement future gas sensing technologies using diverse two dimensional TMDs nanomaterials.

Results

Wafer-scale synthesis of atomic-layered MoS_2. Most approaches use direct/indirect sulphurisation of Mo-containing thin films to synthesise atomic-layered MoS_2 thin films. The precursor is a key factor in the synthesis of MoS_2. In previous studies, most authors adopted one of three precursors: molybdenum thin films[16]; molybdenum trioxide[17]; or ammonium thiomolybdate[18]. However, previous methods have involved complex precursor preparations, yielding films with inconsistent quality. In our search for strategies for synthesising uniform wafer-scale MoS_2 (see schematic in Fig. 1a), we have focused on the development of a thermal CVD system and process. Atomic-layered MoS_2 was grown using molybdenum trioxide (MoO_3) deposited onto a sapphire substrate and a sulphur powder source. The sublimated sulphur served as a precursor to sulphurise the MoO_3 film. To achieve our overall goal of preparing MoS_2 films of consistent quality on the desired substrates, we turned our attention to pressure control during the CVD reaction. A recent report indicated that an increase in the amount of either Mo or S atoms results in increased formation of energetically favourable defects on the MoS_2 surface during film growth[19]. Thus, we systematically controlled the reaction pressure to provide sufficient sublimated sulphur using a custom-made automatic pressure control system (Supplementary Fig. S1).

The new CVD system design was very effective for the uniform synthesis of MoS_2 films on 2-inch sapphire substrates, as illustrated in Fig. 1b. Cross-sectional transmission electron microscopy (TEM) was used to examine the number of layers formed by CVD (Fig. 1c). The MoS_2 films contained double, triple, and, in some cases, more than three layers (additional TEM images, TEM energy-dispersive X-ray spectroscopy (EDS) maps, TEM EDS point spectra, atomic force microscopy images, X-ray photoelectron spectra, and absorption spectra are provided in Supplementary Figs. S2–7). The Raman spectrum in Fig. 1d shows the in-plane vibrational mode of the Mo and S atoms (E_{2g}) and the out-of-plane vibrational mode of S atoms (A_{1g}) in the as-synthesised MoS_2 films[20]. The difference in peak position (Δ) between the E_{2g} and A_{1g} bands, which is a strong indicator of the number of layers, was approximately 22.9. This result indicates that the as-synthesised MoS_2 was mainly composed of three layers[18,21,22]. To confirm the wafer-scale synthesis of MoS_2, we conducted a large-scale structural analysis using Raman mapping and an imaging technique. The Raman mapping area was 50×50 μm^2 with 0.3 μm steps (the original Raman mapping spectra are shown in Supplementary Fig. S8). The corresponding Raman images revealed the spatial distribution of MoS_2 over a 250-μm^2 area of the substrate (Figs. 1e and f). The blue and red models show the spatial distributions of the E_{2g} and A_{1g} bands, respectively. The as-synthesised MoS_2 was highly uniform over a large area of the surface (Figs. 1e and f). Thus, systematic pressure control during the CVD process resulted in highly uniform MoS_2 films on the wafer scale.

Gas detection characteristics of the MoS_2 gas sensor. The uniform atomic-layered MoS_2 films were used for gas molecule detection (Fig. 2a). Transient resistance responses were investigated using two analyte gases (NO_2 or NH_3 at concentrations from 1.2 to 50 ppm). The gas sensitivity was calculated using $\Delta R/R_a = (R_g - R_a)/R_a$, where R_a and R_g represent the resistances of the device to air and the analyte gas, respectively. In the NO_2 gas mode, the resistance increased (positive sensitivity) (Fig. 2b). The NO_2

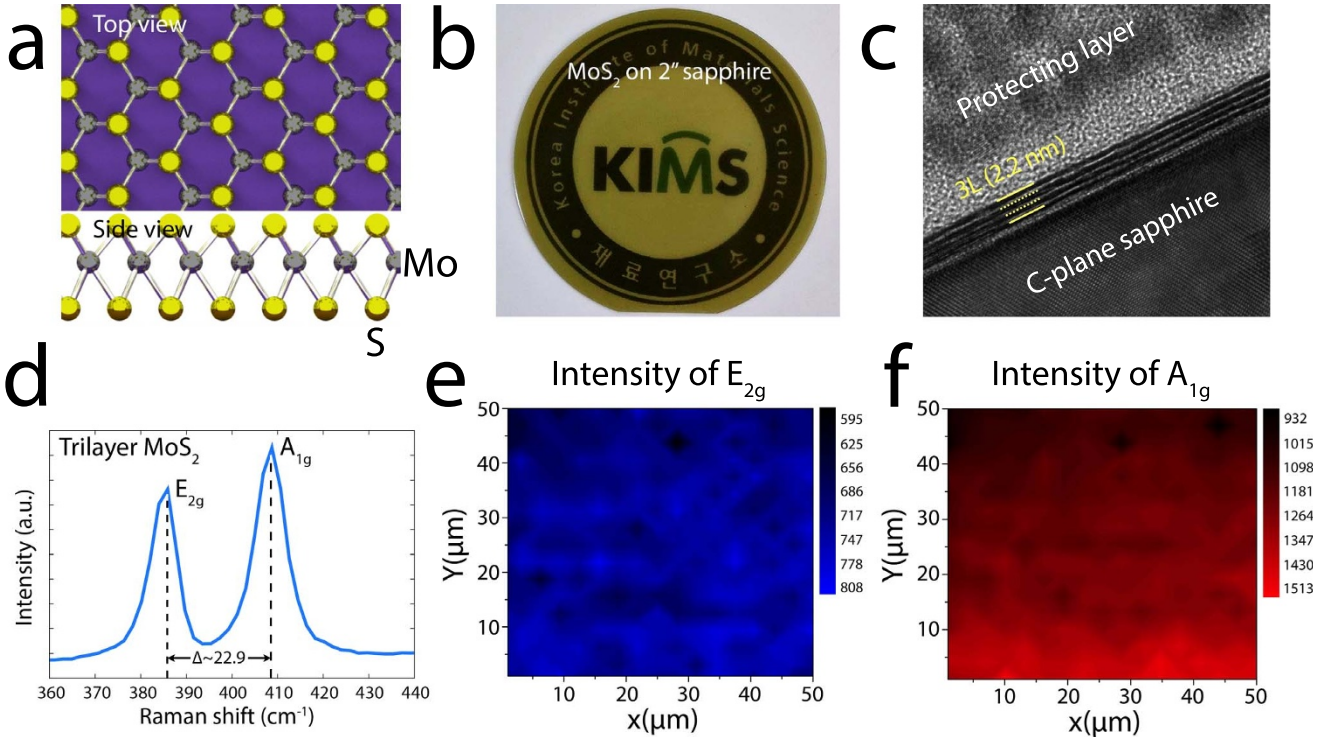

Figure 1 | Large-scale synthesis of MoS_2. (a) Schematic of the atomic-layered MoS_2. The quasi-2D MoS_2 was occupied by one Mo (a trigonal prismatic structure) and two S atoms (hexagonal planes). (b) Image of the as-synthesised MoS_2 film on the 2-inch sapphire substrate. The as-synthesised MoS_2 film was semi-transparent. (c) Cross-sectional TEM images of the as-grown MoS_2 films. The image clearly demonstrates that the synthesised MoS_2 films consisted of three layers of MoS_2. (d) Raman spectrum of the triple-layered MoS_2. The spectrum reveals a strong in-plane vibrational mode for the Mo and S atoms (E_{2g}) and an out-of-plane vibrational mode for the S atoms (A_{1g}). The peak position difference (Δ) between the E_{2g} and A_{1g} bands is approximately 22.9, indicating triple-layered MoS_2. (e, f) Raman maps of E_{2g} (blue) and A_{1g} (red), respectively. The Raman mapping area was 50×50 μm^2 with 0.3 μm steps. The Raman images show the spatial distribution on the surface of the substrates.

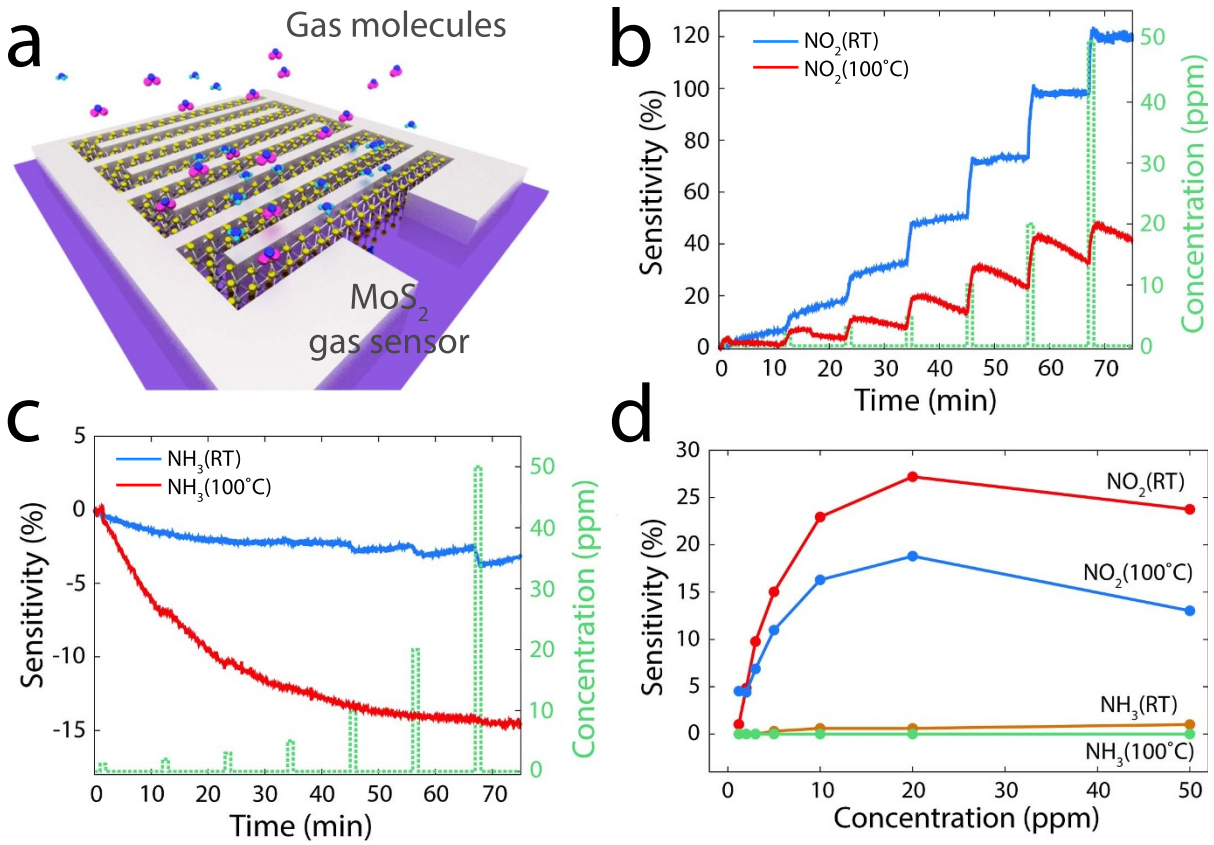

Figure 2 | Gas-sensing using the MoS_2 device. (a) 3D schematic of the MoS_2 gas-sensing device for NO_2 and NH_3. (b) Transient NO_2 gas response at 1.5 to 50 ppm gas at operating temperatures of RT and 100°C. In the NO_2 gas mode, the resistance increases (positive sensitivity). The recovery rate of NO_2 is higher at 100°C than at RT. (c) The transient NH_3 gas response at 1.5 to 50 ppm gas at operating temperatures of RT and 100°C. The resistance decreases with the adsorption of NH_3 gas molecules (negative sensitivity). The NH_3 sensing signal is negligible at 100°C. (d) Comparison of the NO_2 and NH_3 sensitivities at different gas concentrations and operating temperatures. The highest selectivity of NO_2 to NH_3 was obtained when the concentration reached 20 ppm at 100°C.

sensitivity values were comparable to those in a previous report[8]. NO_2 acts as an electron acceptor, resulting in p-doping (Supplementary Fig. S12). The NO_2 molecules on the surface of MoS_2 bring the Fermi level closer to the valence-band edge. During the desorption process, thermal energy (heating to 100°C) enhances the rate of desorption of the NO_2 molecules from the MoS_2 film (Fig. 2b, red line). We next compared the gas sensing characteristics for NH_3 to those for NO_2 (Fig. 2c). In contrast to the resistance recorded for NO_2 molecules, the resistance of the MoS_2 sensing device decreased with the adsorption of NH_3 gas molecules, i.e., negative sensitivity was observed. NH_3 acts as an electron donor (i.e., n-doping) such that it shifts the Fermi level of the MoS_2 to the conduction-band edge. However, theoretical calculations indicated that the Fermi-level shift induced by the NH_3 molecules is negligible (Supplementary Fig. S12). The measured overall NH_3 sensitivities were lower than those of NO_2 (Figs. 2b and c) because of the smaller charge transfer of NH_3 compared to that of NO_2[23]. The dependence of the gas response on the gas concentration at different operating temperatures is plotted in Fig. 2d. The surface chemical reaction between the MoS_2 channel and the NO_2 molecules saturated at approximately 20 ppm, irrespective of the operating temperature (Fig. 2d, red and blue lines). By contrast, in the case of NH_3, the sensitivity at RT gradually increased from 5 to 50 ppm and the sensitivity under 5 ppm was undetectable. However, the sensing signal at 100°C was imperceptible at all concentrations (Supplementary Fig. S9). Thus, the recovery rate of NO_2 at 100°C is clearly superior to that of NH_3, which is closely related to the faster desorption process of NO_2 molecules as a result of the thermal energy[24,25]. At 20 ppm and 100°C, we obtained the best selectivity for NO_2 relative to NH_3 (~400% increase compared to that at RT).

***In situ* photoluminescence of the MoS_2-based gas sensor.** To explore the gas adsorption characteristics of the MoS_2, we adopted theoretical and experimental approaches. First-principles density functional theory (DFT) calculations were conducted using the screened hybrid functional of Heyd-Scuseria-Ernzerhof with the D2 correction for van der Waals interactions[26,27] (see the detailed methods in the Supplementary Information). To simulate NO_2 and NH_3 adsorption onto the MoS_2 monolayer, supercells containing 16 Mo and 32 S atoms with NO_2 and NH_3 were employed using a $2 \times 2 \times 1$ k-point grid. The most stable configurations of NO_2 and NH_3 reported in a recent study that compared the total energy between different adsorption configurations[28] were considered. The NO_2 and NH_3 molecules were preferentially adsorbed onto the top of the hexagon of the MoS_2[28] (Figs. 3a and b). The adsorption energies of the NO_2 and NH_3 gas molecules were evaluated using $E_a = E_{(MoS_2-molecule)} - \left[E_{(MoS_2)} + E_{(molecule)}\right]$, where $E_{(MoS_2-molecule)}$ is the total energy of a supercell containing both an MoS_2 monolayer and a gas molecule (NO_2 or NH_3), $E_{(MoS_2)}$ is the total energy of the host MoS_2 supercell, and $E_{(molecule)}$ is the total energy of a supercell containing a gas molecule. The calculated adsorption energies of NO_2 and NH_3 were −0.14 eV and −0.16 eV, respectively. These values were ~0.1 eV smaller than the values obtained using the local density approximation (LDA) because the LDA functional overestimates the adsorption energy[28]. The negative adsorption energies indicate that the adsorption process is exothermic. Thus,

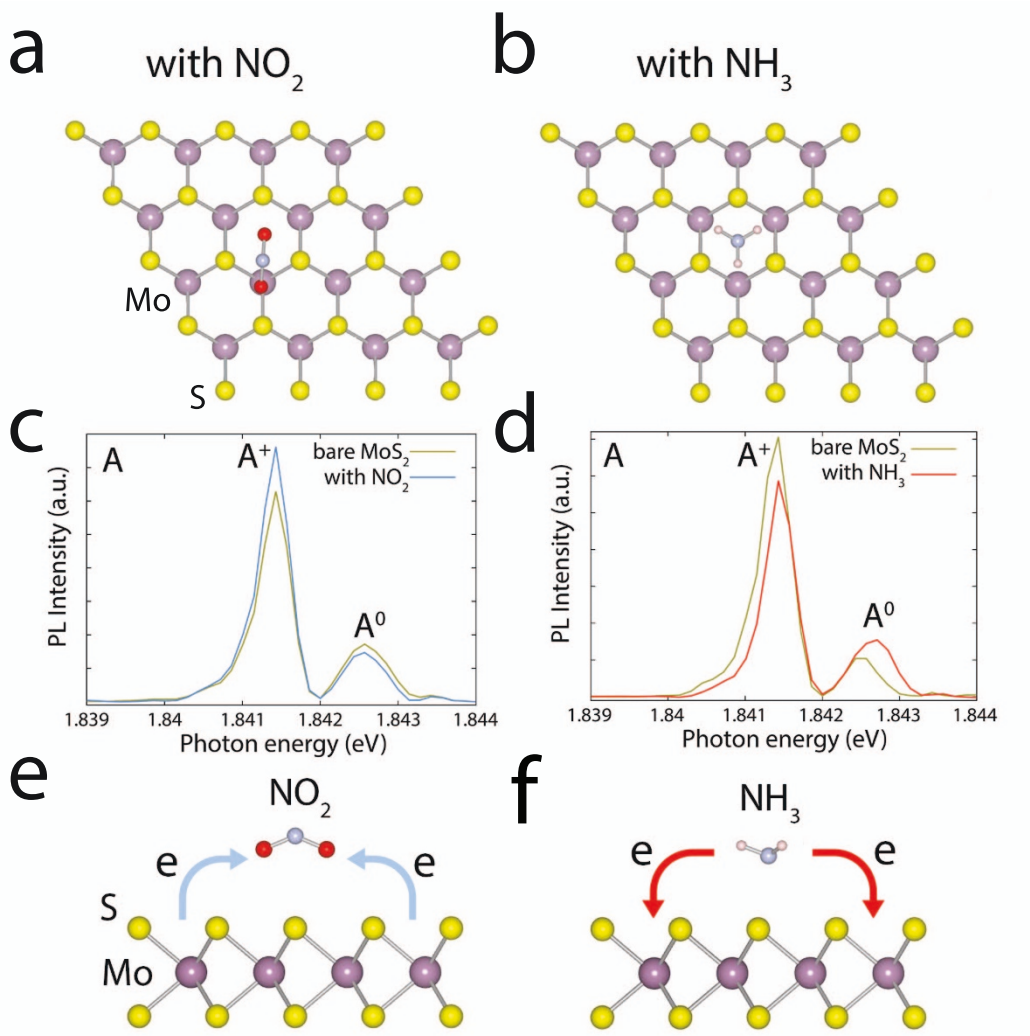

Figure 3 | Adsorption configurations and *in situ* PL. (a, b) Top views of the most favourable configurations for NO_2 (a) and NH_3 (b) on the MoS_2. The calculated adsorption energies were −0.14 eV for NO_2 and −0.16 eV for NH_3. The negative adsorption energies indicate that the adsorption process is exothermic, indicating that NO_2 and NH_3 molecules are likely to be adsorbed onto the surface of the MoS_2. (c, d) *In situ* PL spectra recorded from the MoS_2 with NO_2 (c) and NH_3 (d) molecules. The overall intensity of the PL spectra changes in the presence of NO_2 and NH_3 molecules. The PL intensities of the A^+ trions and A^0 excitons are either suppressed or increased by changes in the concentrations of the charge carriers. (e, f) Schematics of the charge density differences for MoS_2 in the presence of NO_2 (e) and NH_3 (f) gas molecules. NO_2 molecules on the surface of MoS_2 act as electron acceptors, whereas NH_3 molecules act as electron donors.

NO_2 and NH_3 molecules are likely to be adsorbed onto the surface of MoS_2.

Next, we turned our attention to the *in situ* characterisation of PL to study the sensing mechanism in depth. The high temperature during film growth can induce unintentional defects on the substrate/MoS_2 interface. To prevent defects, we transferred the as-grown MoS_2 from the sapphire substrate to a SiO_2/p + Si substrate. Interestingly, the atomic-layered MoS_2 transferred onto the SiO_2/p + Si substrate exhibited opposite gas sensitivity (i.e., p-type behaviour) compared to the n-type behaviour of MoS_2 on the sapphire substrate (see Supplementary Fig. S13 for details). Dangling bonds at the semiconductor/substrate interface can redefine the effective Fermi levels within gap states, modulating the conductive properties of the MoS_2[29]. The dangling oxygen bonds on the SiO_2 surface can result in a p-type MoS_2 semiconductor[29]. In the *in situ* PL characterisation with the two analyte gases (see Supplementary Fig. S10 for details), we observed various intensity changes in the PL spectra for NO_2 and NH_3 molecules (Figs. 3c and d). The atomic-layered MoS_2 had two main PL peaks associated with the A and B excitons[30] (Supplementary Figs. S11). Spin-orbit coupling-induced valence-band splitting can give rise to A and B excitons[31]. After the gas molecules are adsorbed, the PL intensities of the A and B excitons can either be suppressed or increased by changing the concentrations of the charge carriers[32,33]. We here focused on the signal peak of the A exciton. The relatively low-energy A exciton signal expands to two features: a trion of $A^{-/+}$ (two electrons to a hole, resulting in a negatively charged exciton, or an electron to two holes, resulting in a positively charged exciton) and a neutral exciton of A^0 [32,33]. With the emergence of the trion, we assumed that the exciton is coupled to either another electron or to a hole at the Fermi level. In the case of MoS_2, the A^+ and A^0 peaks correspond to the trions (1.8413 eV) and to the neutral excitons (1.8424 eV), respectively. The bare MoS_2 notwithstanding, the positive trion (in this case, an electron to two holes, resulting in positively charged excitons, A^+) emission dominates the PL spectra because the bare MoS_2 on the SiO_2 substrate exhibits p-type characteristics, as previously mentioned[32]. As schematically shown in Fig. 3e, the NO_2 molecules on the surface of the MoS_2 act as electron acceptors (p-type dopants), whereas the NH_3 molecules act as electron donors (n-type dopants)[28]. By adsorp-

tion of NO_2 gas molecules, a neutral exciton (A^0) can be converted into a quasi-particle (A^+) because of excessive holes generated by electron extraction from the MoS_2[34]. As a result, the A^+ peak in the PL spectrum increases in intensity and the A^0 peak is suppressed (Fig. 3c). By contrast, when additional electrons are introduced from the NH_3 molecules, the intensity of the A^+ peak in the PL spectrum is suppressed because of dissociation of the positive trions from the neutral excitons, resulting in increasing neutral excitons (A^0)[35], as shown in Fig. 3d. The *in situ* PL characterisation clarifies the mechanisms of charge transfer between the MoS_2 and the gas molecules.

Discussion

The gas sensing characteristics of wafer-scale layered MoS_2 fabricated by CVD were determined. The gas sensor based on the CVD-fabricated MoS_2 exhibited excellent sensitivity and high selectivity. The *in situ* PL characterisation and theoretical studies elucidated the charge-transfer mechanism between the gas molecules and the MoS_2. In-depth PL studies verified that the electron depletion of the MoS_2 by NO_2 adsorption increased the intensity of the A^+ peak and suppressed that of the A^0 peak, whereas electron accumulation by NH_3 adsorption suppressed the intensity of the A^+ peak and increased that of the A^0 peak. Intensive PL characterisation clarified the charge transfer phenomena between the MoS_2 and the gas molecules. The results of this study will enable more extensive applications of gas sensing using two dimensional transition metal dichalcogenides nanomaterials.

Methods

CVD synthesis of the MoS_2 nanofilms. MoS_2 nanofilms were synthesised using chemical vapour deposition (CVD) (Teraleader Co., Ltd., South Korea) (Supplementary Fig. S1). First, C-plane sapphire substrates were prepared using a typical cleaning process (sonication in acetone, isopropyl alcohol, and deionised water for 10 min each). MoO_3 films (5 nm) were deposited onto the clean substrates using a thermal evaporator. The pre-deposited MoO_3 samples were placed at the centre of the furnace, and ~1 g of sulphur powder, which was used as a sulphur precursor, was subsequently loaded into a quartz boat in an independently temperature-controllable flange heater located near the inlet of the furnace. The furnace and the flange heater were heated to ~850°C and ~180°C, respectively, for 1 h. The process was maintained for an additional 1 h under flowing Ar/H_2 gas (volume ratio: $Ar : H_2 = 85 : 15\%$) at a chamber pressure of 760 torr. The MoO_3 film was converted into a MoS_2 nanofilm via a two-step reaction (the reduction of MoO_3 by hydrogen gas, followed by sulphurisation of the reduced MoO_3 with sublimated sulphur gases). Finally, the furnace was rapidly cooled to room temperature by opening the chamber box after the furnace was turned off.

Fabrication of the MoS_2 sensing device. The SiO_2 (300 nm)/C-plane sapphire was cleaned using a typical cleaning process (sequential sonication in acetone, isopropyl alcohol, and deionised water for 10 min each). A MoO_3 film (~5 nm thick) was patterned with an active shadow mask using a thermal evaporator. The patterned MoO_3 film was converted into a MoS_2 nanofilm by CVD. Using a thermal evaporator and a shadow mask with an interdigitated electrode array structure consisting of two opposing comb-shaped electrodes with a width of 400 μm and a gap of 100 μm, we deposited an Ag film (100 nm; used for the electrodes) onto the MoS_2 nanofilm. Detailed fabrication schemes are provided in Supplementary Fig. S14.

Characterisation of CVD-synthesised MoS_2, gas sensing, DFT calculations, *in situ* PL tests. See the detailed methods in the Supplementary Information.

1. Fine, G. F., Cavanagh, L. M., Afonja, A. & Binions, R. Metal oxide semi-conductor gas sensors in environmental monitoring. *Sensors (Basel).* **10**, 5469–5502 (2010).
2. Pearton, S. J. *et al.* Recent advances in wide bandgap semiconductor biological and gas sensors. *Prog. Mater. Sci.* **55**, 1–59 (2010).
3. Huang, J. & Wan, Q. Gas sensors based on semiconducting metal oxide one-dimensional nanostructures. *Sensors (Basel).* **9**, 9903–9924 (2009).
4. Kong, J. Nanotube Molecular Wires as Chemical Sensors. *Sience* **287**, 622–625 (2000).
5. Schedin, F. *et al.* Detection of individual gas molecules adsorbed on graphene. *Nat. Mater.* **6**, 652–655 (2007).
6. Late, D. J. *et al.* Sensing Behavior of Atomically Thin-Layered MoS_2 Transistors. *ACS Nano* **7**, 4879–4891 (2013).
7. Li, H. *et al.* Fabrication of single- and multilayer MoS_2 film-based field-effect transistors for sensing NO at room temperature. *Small* **8**, 63–67 (2012).
8. He, Q. *et al.* Fabrication of flexible MoS_2 thin-film transistor arrays for practical gas-sensing applications. *Small* **8**, 2994–2999 (2012).
9. Lee, K., Gatensby, R., McEvoy, N., Hallam, T. & Duesberg, G. S. High Performance Sensors Based on Molybdenum Disulfide Thin Films. *Adv. Mater.* **25**, 6699–6702 (2013).
10. Yao, Y. *et al.* High-concentration aqueous dispersions of MoS_2. *Adv. Funct. Mater.* **23**, 3577–3583 (2013).
11. Perkins, F. K. *et al.* Chemical vapor sensing with monolayer MoS_2. *Nano Lett.* **13**, 668–673 (2013).
12. Wang, Q. H., Kalantar-Zadeh, K., Kis, A., Coleman, J. N. & Strano, M. S. Electronics and optoelectronics of two-dimensional transition metal dichalcogenides. *Nat. Nanotechnol.* **7**, 699–712 (2012).
13. Ganatra, R. & Zhang, Q. Few-Layer MoS_2: A Promising Layered Semiconductor. *ACS Nano* **8**, 4074–4099 (2014).
14. Jariwala, D., Sangwan, V. K., Lauhon, L. J., Marks, T. J. & Hersam, M. C. Emerging Device Applications for Semiconducting Two-Dimensional Transition Metal Dichalcogenides. *ACS Nano* **8**, 1102–1120 (2014).
15. Radisavljevic, B., Radenovic, A., Brivio, J., Giacometti, V. & Kis, A. Single-layer MoS_2 transistors. *Nat. Nanotechnol.* **6**, 147–150 (2011).
16. Lee, Y. *et al.* Synthesis of wafer-scale uniform molybdenum disulfide films with control over the layer number using a gas phase sulfur precursor. *Nanoscale* **6**, 2821–2826 (2014).
17. Lin, Y.-C. *et al.* Wafer-scale MoS_2 thin layers prepared by MoO_3 sulfurization. *Nanoscale* **4**, 6637–6641 (2012).
18. Liu, K.-K. *et al.* Growth of large-area and highly crystalline MoS_2 thin layers on insulating substrates. *Nano Lett.* **12**, 1538–1544 (2012).
19. Najmaei, S. *et al.* Vapour phase growth and grain boundary structure of molybdenum disulphide atomic layers. *Nat. Mater.* **12**, 754–759 (2013).
20. Bertrand, P. A. Surface-phonon dispersion of MoS_2. *Phys. Rev. B* **44**, 5745–5749 (1991).
21. Li, S. *et al.* Quantitative raman spectrum and reliable thickness identification for atomic layers on insulating substrates. *ACS Nano* **6**, 7381–7388 (2012).
22. Liu, Y. *et al.* Layer-by-layer thinning of MoS_2 by plasma. *ACS Nano* **7**, 4202–4209 (2013).
23. Yue, Q., Shao, Z., Chang, S. & Li, J. Adsorption of gas molecules on monolayer MoS_2 and effect of applied electric field. *Nanoscale Res. Lett.* **8**, 425 (2013).
24. Yavari, F. *et al.* High sensitivity gas detection using a macroscopic three-dimensional graphene foam network. *Sci. Rep.* **1**, 166 (2011).
25. Choi, H. *et al.* Flexible and transparent gas molecule sensor integrated with sensing and heating graphene layers. *Small* **10**, 3812 (2014).
26. Heyd, J., Scuseria, G. E. & Ernzerhof, M. Hybrid functionals based on a screened Coulomb potential. *J. Chem. Phys.* **118**, 8207–8215 (2003).
27. Krukau, A. V., Vydrov, O. a., Izmaylov, A. F. & Scuseria, G. E. Influence of the exchange screening parameter on the performance of screened hybrid functionals. *J. Chem. Phys.* **125**, 224106 (2006).
28. Yue, Q., Shao, Z., Chang, S. & Li, J. Adsorption of gas molecules on monolayer MoS_2 and effect of applied electric field. *Nanoscale Res. Lett.* **8**, 425 (2013).
29. Dolui, K., Rungger, I. & Sanvito, S. Origin of the n-type and p-type conductivity of MoS_2 monolayers on a SiO_2 substrate. *Phys. Rev. B* **87**, 165402 (2013).
30. Splendiani, A. *et al.* Emerging photoluminescence in monolayer MoS_2. *Nano Lett.* **10**, 1271–1275 (2010).
31. Coehoorn, R., Haas, C. & de Groot, R. A. Electronic structure of $MoSe_2$, MoS_2, and WSe_2. II. The nature of the optical band gaps. *Phys. Rev. B* **35**, 6203–6206 (1987).
32. Mak, K. F. *et al.* Tightly bound trions in monolayer MoS_2. *Nat. Mater.* **12**, 207–211 (2013).
33. Mouri, S., Miyauchi, Y. & Matsuda, K. Tunable photoluminescence of monolayer MoS_2 via chemical doping. *Nano Lett.* **13**, 5944–5948 (2013).
34. Ross, J. S. *et al.* Electrical control of neutral and charged excitons in a monolayer semiconductor. *Nat. Commun.* **4**, 1474 (2013).
35. Mao, N., Chen, Y., Liu, D., Zhang, J. & Xie, L. Solvatochromic effect on the photoluminescence of MoS_2, monolayers. *Small* **9**, 1312–1315 (2013).

Acknowledgments

This study was supported financially by the Fundamental Research Program (PNK3770 and PNK4060) of the Korean Institute of Materials Science (KIMS) and by the "Gyeongsangnam, Changwon Science Research Park Project" of the Grant of the Korean Ministry of Science, ICT and Future Planning. M. G. H. and B. C. are grateful for support from the Basic Science Research Program of the National Research Foundation of Korea (NRF) funded by the Ministry of Science, ICT & Future Planning (NRF-2014R1A1A1006214 and NRF-2014R1A1A1036139). MC was supported by Global Frontier Program through the Global Frontier Hybrid Interface Materials (GFHIM) of the National Research Foundation of Korea (NRF) funded by the Ministry of Science, ICT & Future Planning (2013M3A6B1078872).

Author contributions

B.C., M.G.H. and D.-H.K. designed and supervised the experiments. B.C., M.G.H. and A.R.K. synthesised the MoS_2. B.C., M.G.H., J.Y., A.R.K. and Y.-J.L. characterised the MoS_2. B.C. and A.R.K. fabricated the MoS_2-based devices. B.C., M.G.H., S.L., T.J.Y. and C.G.K. measured the MoS_2 sensing devices. M.G.H. and M.C. performed the first-principles DFT

calculations for the MoS_2 with gas molecules. B.C., M.G.H., M.C., S.-G.P., J.-D.K., C.S.K., M.S., Y.J., K.-S.N., B.H.L., H.C.K., P.M.A. and D.-H.K. analysed the data. B.C., M.G.H. and D.-H.K. co-wrote the paper. All authors discussed the results and commented on the manuscript.

Additional information

Supplementary information accompanies this paper at http://www.nature.com/scientificreports

Competing financial interests: The authors declare no competing financial interests.

How to cite this article: Cho, B. *et al.* Charge-transfer-based Gas Sensing Using Atomic-layer MoS_2. *Sci. Rep.* **5**, 8052; DOI:10.1038/srep08052 (2015).